JOURNAL OF OPTOELECTRONICS AND ADVANCED MATERIALS Vol. 8, No. 4, August 2006, p. 1456 - 1459

Electrical and optical properties of Cr nano-crystal/silicon ultra-thin films prepared by electrodeposition

V. GEORGESCU, C. SÎRBU, N. APETROAIEI
Faculty of Physics, Al. I. Cuza University, Iasi, RO-700506 Romania

Electronic transport properties of ultra-thin films and of nanometer-sized crystallites of metals deposited onto semiconductors play an important role for the development of nanoscaled electronic devices. In this work, we report the electrical and optical properties of ultra-thin films (2 nm ÷ 150 nm) composed of Cr nano-crystals electrodeposited onto n-Si (100) phosphorous-doped single crystal. The films were prepared by an electrochemical procedure using for electrodeposition a solution based on CrO_3. Three-dimensional metallic Cr nano-crystals grow over Si substrate according to a Volmer-Weber mechanism, as was evidenced by AFM measurements. The analysis of photo-resistance for a series of samples deposited for various charge densities allows us to detect the onset of metallic conductivity due to the percolation of island-like Cr metal films on the semiconductor substrate.

(Received May 8, 2006; accepted July 20, 2006)

Keywords: Electrodeposition, Metallic films, Atomic force microscopy, Surface structure, Photoconductivity

1. Introduction

Metal/silicon interfaces have received much recent attention due to their growing demand in microelectronic technology. Research concerning the interaction between silicon or silicon oxide and metals is of greatest interest due to the use of silicon as the main constituent in electronic device technology, and the necessity to make good ohmic contacts with metallic conductors or to obtain photo-electrochemical cells [1- 6]. The Cr/Si system is of special interest due to the extremely high stability of the chromium silicides [7].

Przenioslo et al. [8, 9] studied the magnetic ordering in electrodeposited Cr foils with nanocrystalline grains. It was shown that the reduced crystallite size has a strong influence on the electronic and magnetic properties of nanocrystalline Cr. Similar studies of nanocrystalline Cr prepared by other methods were published by Tsunoda et al. [10] for inert gas condensation and Ishibashi et al. for plasma metal reaction method [11]. The magnetic ordering of Cr single crystals is of antiferromagnetic type superposed to a spin density wave with a period of about 6.5 nm; for polycrystalline Cr above room temperature there is a simple antiferromagnetic ordering.

Many metals have been deposited onto silicon so far by various methods. The electrodeposition is a low expensive procedure, working at room temperature, which could lead to the integration of this method for fabricating thin layers, with silicon technology. Due to low adherence of ferromagnetic transition metals onto silicon, we have chosen to investigate the electrodeposition of Cr onto a silicon wafer with a view to use this system as a buffer layer for magnetic Co or Fe electrodeposition. The choice for depositing Cr onto silicon is a point to consider when Co-Cr or Fe-Cr alloys/multilayers growth is envisaged (these systems are known for GMR applications). Electrodeposition of such thin films and multilayers directly on semiconductors is a subject of fundamental and practical significance. Although chromium is an important material used by the electroplating industry, the electrodeposition of Cr onto silicon substrate is lacking, since, to our knowledge. Therefore, we investigate here the electric and optical properties of the Cr films for the early stages of the electrodeposition onto silicon wafer substrate.

2. Experimental

For the current research, one-side polished n-Si (100) samples (phosphorous-doped, less than $1\,\Omega$cm specific resistance, 0.375-μm thickness) were used as support for electrodeposition of Cr ultra thin films. Electrodeposition was performed in a dark chamber in a conventional cell. The Pt foil counter electrode was placed directly opposite the working electrode (substrate). Ohmic contacts to each substrate were made through silver paste back contact. A holder from Teflon was used to fix the samples.

Surface analyses were performed using an atomic force microscope (AFM) in tapping mode, at room temperature and with a commercial Si_3N_4 tip of radius 10 nm.

Reflection spectra for ultra-thin Cr/Si films with various thicknesses were recorded in the photon energy range 1.18 – 3.1 eV using a computer controlled STEAG-ETA Optic Spectrometer.

The measurements of surface resistance (R) of the samples were carried out with an HM 8112-2 programmable multimeter, in current in plane (CIP) geometry with two pressure gold contacts (at a distance of 8 mm each another), using a load-independent current of I=7 μA passing trough the resistance R which is to be measured. The polarity of the current flowing through R may be changed. The voltage drop across R is measured, and the ratio of this voltage drop to I is calculated. The correction for all possible sources of errors is made compensates automatically, by construction.

3. Results and discussion

3.1. Sample preparation

Cleaning procedure for the silicon substrate consisted in three steps: a) degreasing for about 2 h by refluxing in isopropanol, b) cleaning by boiling in a 1: 1: 5 volume

mixtures of NH_3, H_2O_2 and H_2O, and c) cleaning in a 1: 1: 5 volume mixtures of HCl, H_2O_2 and H_2O at about 80 °C.

Preceding the deposition of Cr, the Si samples were immersed for 1 min into 50% HF to remove the oxide layer and then for 3 min in 40% NH_4F solution. By this procedure, hydrogen-terminated Si surfaces were prepared [12].

For the electrodeposition of Cr ultra thin films, the electrolytic bath contained CrO_3 (250 g/l) and H_2SO_4 (1 ml/l) in double distilled water. The temperature of the electrolyte remained at (65 ± 1) ^oC during the electrodeposition. The charge density passing through electrolyte during electrodeposition was modified as to obtain a series of samples with different thickness, maintaining the other working parameters at a suitable fixed value.

3.2. AFM characterization

Atomic force microscopy has been employed to investigate the morphology of ultra-thin Cr films grown by this method on n-type Si (100) substrate phosphorus doped. The measurements were used to investigate the influence of the charge density passing through electrolyte during electrodeposition on the film morphology, for the series of samples prepared with different charge density.

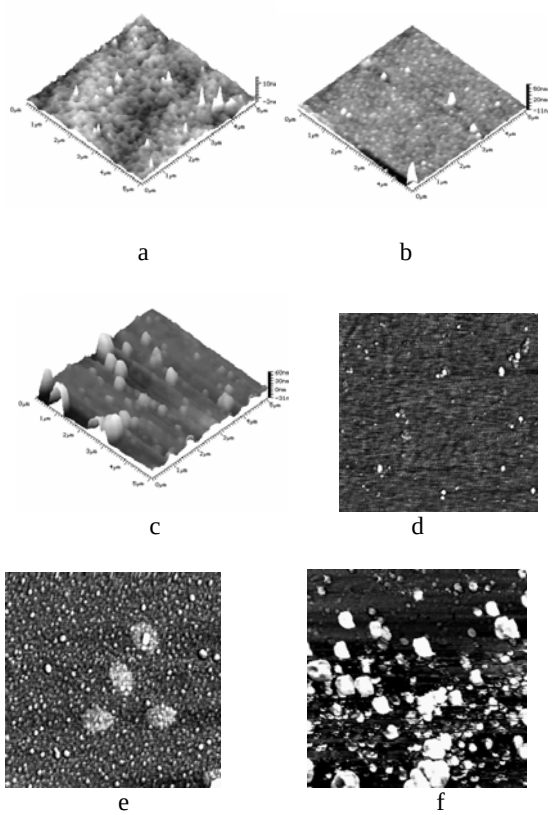

Fig. 1. Topographical AFM images (top row) and phase images (bottom row) for some samples deposited at a charge density of a) 21.6 C.cm^{-2}, b) 76.2 C.cm^{-2} and c) 204.0 C.cm^{-2}. All scans are 5 μm. The height scale is 17 nm for images (a, d), 71 nm for (b, e) and 91 nm for (c, f).

AFM images of some typical samples electrodeposited for various charge densities are presented in Fig. 1. Topographical 3D AFM images (top row, images a, b and c) and phase images (bottom row, images d, e an f) are shown for the samples deposited at a charge density of: 21.6 C.cm^{-2} (a, d), 76.2 C.cm^{-2} (b, e) and 204.0 C.cm^{-2} (c, f), respectively. From the general inspection of these images, it is evident that Cr deposited on the silicon surface following a progressive nucleation process. The deposit consisted in spatially scattered fine particles in all cases when the charge density was lower than 200 C.cm^{-2}. An increase in the charge density passing across the electrode surface led to an increase in the size and in the density of insular Cr nano-crystal.

For the series of samples electrodeposited with different charge density, the roughness parameter - root mean square (*RMS*) was calculated from AFM topographic images. The results are presented in figure 2, showing the dependence of *RMS* parameter on charge density (*Q*) for these samples. It can be seen from the curve in fig. 2 that as the current density increases, the roughness become larger. When the charge density was smaller than 200 C.cm^{-2}, a uniform coating could not be produced on the substrate, the deposition consisting in small nanocrystalline grains only. We estimated the number (*N*) of mono-atomic layers (ML) in such a nano-crystal considering the Cr atomic radius of 0.128 nm**.** Therefore, for the three samples exemplified in Fig. 1, the estimated mean numbers of mono-atomic layers were of 11 ML, 45 ML and 124 ML, respectively.

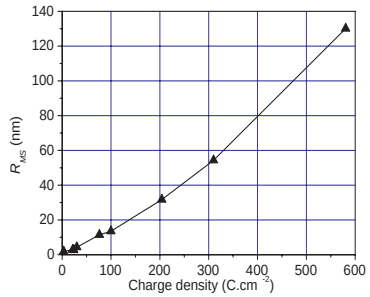

Fig. 2. Mean square roughness of some samples as a function of the charg e density (Q) applied during their preparation.

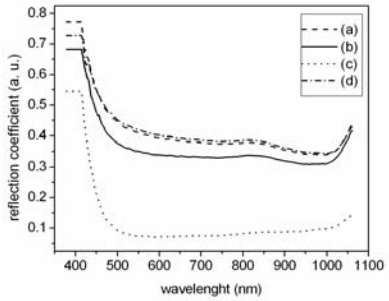

Fig. 3. Reflection spectra for Cr samples deposited onto n-Si (100) phosphorus doped, in the case of nano-crystals with: a) N=17 ML, b) N=124 ML c) N=508 ML, in comparison with the reflection spectra of the substrate (d).

From AFM images, it can be seen that three-dimensional Cr particles grow after nucleation over Si substrate according to a Volmer-Weber mechanism, with an average size depending on *Q*. We have found also that the average size of the Cr particles increased with the charge density passed through electrolyte. The results of Figs. 1 and 2 clearly show that the size and distribution density of Cr particles on n-Si can be controlled by changing the charge density passed through cathode/electrolyte interface.

3.3 Optical properties

In order to characterize the optical properties of the samples, the reflection spectra for the series of Cr/Si samples were measured with computer controlled STEAG-ETA optic spectrometer and presented in Fig. 4. The spectra were recorded in the photon energy range 1.18–3.1eV, using an Aluminum sheet as reference. We have found a decrease of reflection coefficient with the wavelength within spectral domain 450 – 750 nm, both for n-Si phosphorous-doped (curve d in figure 3) and for Cr nano-crystals/n-Si (curves a, b and c in figure 4, for N=17 ML, 124 ML and 508 ML, respectively). This behaviour is enhanced by the presence of Cr nano-crystals; it is probably due to the increase in the absorption coefficient for thicker Cr layers. One can observe a bump at around 810 nm (cf. Fig. 4) characteristic for Si and for the samples incompletely covered with Cr nano-crystals (*N*= 17, *N*=124). The Cr spectrum (for *N* = 508 ML) is relatively flat between 550 nm and 1000 nm.

3.4. Electric behaviour

Electric behaviour of the samples was examined by means of photo-resistance measurements. Direct-current measurements were carried out in current in plane geometry for the series of samples electrodeposited with different *Q*. The experiments were performed in two ways: in a dark chamber and exposing the samples in light (Λ=632.8 nm, 3 mW power on the sample surface). The dependence of planar resistance of the samples on the time was measured in the constant-current mode, at room temperature. Photo-induced transport (measured at fixed time intervals of 30 s) reflects changes in the conductance as a function of time and the nature of the sample. In figure 4 we present the curves of time dependence of the resistance *R* for the samples with N=11 ML (a) and N=508 ML (b). Curves denoted D were registered in the dark and curves denoted L were registered in light. The measurements for the two polarities of the current passing between the point contacts were labelled (1) and (2) in Fig. 4. These curves had an asymmetrical shape with respect to the polarity of the voltage applied, which is an indication about the rectifying character of the contacts formed by deposition of Cr nano-crystals onto the silicon surface. In the first minutes of an experiment, there is a transient regime for photo-resistance, which stabilizes after a longer exposure.

In our experiments, in the samples having the Si surface entirely covered with a Cr film, the photoresistance *R* had lower values than in samples partially covered. For example, the photo-resistances for the samples with N=11 ML (Fig. 4a) and N=508 ML (Fig. 4b) are of the order of 2000 kΩ and 17Ω, respectively. There is a good concordance between electric and optic behaviour: the low resistance metallic samples display the lowest reflection coefficient. When *R* become independent of the polarity of current (ohmic contact), metallic conductivity is established due to the percolation of island-like Cr metal films on the semiconductor substrate.

When the Si surface is covered with metal nano-crystals of several monolayers, it is possible that electric behaviour is dominated by the specific features of such array of nano-crystals (like quantum dots). Thus, the complicated shape of experimental curves *R*(*t*) is caused by the presence of two types of localized states, over which the hopping conduction of electrons takes place. The total resistance of these nanostructures combines from two parallel resistance nets, the resistances of which depend differently on the excitation light. These features are connected with the shape and density of such quantum dots on the sample surface. There is a competition between metallic type conduction in Cr isolated islands and semiconductor n-type conduction through inter-grain spaces; this could explain the shape of curves in Fig. 4 (a) and (b). The photoconductivity depends on both the density and size of the Cr particles. The resistance measured between the two gold contacts in the film plane depends upon the number, geometry and density of the Cr nano-crystals. The surface resistance decreases when the density and size of the Cr particles decreased. The intensity of light on the surface of n-Si is reduced by the presence of Cr nano-crystals. This reduction is related to the area of the n-Si surface covered with the Cr particles. Accordingly, the photoconductivity depends on both the density and size of the Cr particles.

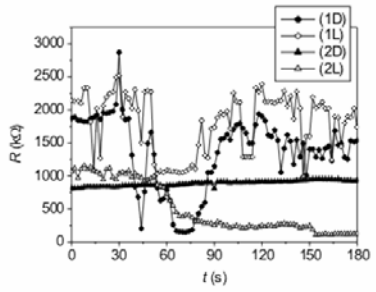

a

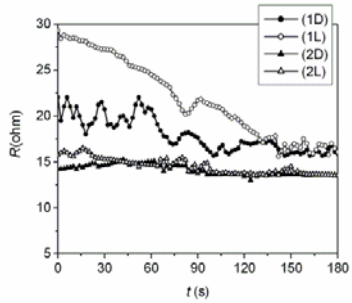

b

Fig. 4. Time dependence of the resistance R for the samples with N=11 ML (a) and N=508 ML (b). Curves denoted D were registered in the dark. Curves labelled L were registered in light (Λ=632.8 nm, 3 mW power on the sample surface). The two polarities of the current passing between the two golden point contacts were labelled (1) and (2).

The low voltage electron transport through an array of metal islands on semiconductor substrate is dominated by the energy required to charge electrically the individual islands [3]. Models of electrical conduction in such an array of metal islands predict a thermally (or light) activated behaviour, with conductance $G=1/R$ expressed as

$$G = G_o \exp[-E_a / k_B T] \quad (1)$$

where, G_0 is the zero bias conductance, E_a is the activation energy to charge an electrically neutral nano-crystals and k_B is Boltzmann's constant. The coulomb charging energy is $E_a=e^2/cC_0$, where $C_0=4\pi\varepsilon_0\varepsilon r$, the capacitance of an isolated Cr nano-crystals, depends on the dielectric constant ε of the surrounding Si medium and the nano-crystal radius r.

Giving the spacing and sizes of the nano-crystals, we suppose that quantum size effects are important in the carrier transport amongst such quantum dots. We observed charge storage and transport behaviour that is completely different for different samples, the photo-resistance characteristics being dominated by electron transport involving nano-crystals.

4. Conclusions

In this study, optical and electrical results were reported on the Cr nano-crystalline ultra-thin films deposited onto n-type Si (100) phosphorus doped substrate and the procedure for electrodeposition from an aqueous CrO_3 solution was established. We examined films deposited for different charge density, with convenient fixed electrodeposition parameters. The charge density passing across the electrode surface during electrodeposition controls the size and the distribution density of insular Cr nano-crystal. The size and the number of monoatomic layers in electrodeposited Cr nano-crystals can be controlled by changing the charge density in the electrodeposition. The very interesting optical and photoelectric properties of chromium nano-crystals/n-type Si make such ultra thin films useful for applications in the domain of functional micro- or nanoscaled devices.

References

[1] M. G. Garnier, T. De los Arcos, J. Boudaden, P. Oelhafen, Surface Science **536**, 130 (2003).
[2] A. Aranz, C. Palacio, Surface Science **588**, 92 (2005).
[3] K. Yang, H. Fan, K. J. Malloy, C. J. Brinker, Th. W. Sigmon, Thin Solid Films **491**, 38 (2005).
[4] M. Gruyters, Surface Science **515**, 53 (2002).
[5] S. Yae, M. Kitagaki, T. Hagihara, Y. Miyoshi, H. Matsuda, B. A. Parkinson, Y. Nakato, Electrochimica Acta **47**, 345 (2001).
[6] F. Raissi, N. A. Sheeni, Sensors and Actuators A **104**, 117 (2003).
[7] R. Przenioslo, J. Wagner, H. Natter, R. Hempelmann, W. Wagner, J. Alloys & Compds. **328**, 259 (2001).
[8] R. Przenioslo, I. Sosnowska, G. Rousse, R. Hempelmann, Phys Rev. **B66**, 014404 (2002).
[9] Y. Tsunoda, H. Nakano and S. Matsuo, J. Phys.: Condens. Matter **5**, L29 (1993).
[10] H. Ishibashi, K. Nakahigashi and Y. Tsunoda, J. Phys.: Condens. Matter **5**, L415 (1993).
[11] O. A. Utas, T. V. Utas, V. G. Kotlyar, A. V. Zotov, A. A. Saranin, V. G. Lifshits, Surface Science **596**, 53 (2005).
[12] J. Zegenhagen, F. U. Renner, A. Reitzle, T. L. Lee, S. Warren, A. Steirle, H. Dosch, G. Scherb, B. O. Fimland, D. M. Kolb, Surface Science **573,** 67 (2004).

*Corresponding author: vgeor@uaic.ro